Aircraft Noise and Performance Data for a Notional Supersonic Business Jet

Jeffrey J. Berton*
NASA Glenn Research Center, Cleveland, Ohio 44135

The International Civil Aviation Organization recently completed a study that determined the global environmental impact of adding several hypothetical supersonic aircraft types to the existing subsonic fleet. NASA supported this study by designing a notional 55-tonne supersonic business jet. The airplane is named the Supersonic Technology Concept Aeroplane by the international community. Performance, noise, and exhaust emission predictions for this transport were used to inform development of new environmental standards for future supersonic civil aircraft. The behavior of the aircraft in an operational setting is considered. Calculation of aircraft noise and performance data for this aircraft is the focus of this paper. Noise abatement departure procedures, stage length performance, and noise-power-distance data are determined using NASA tools. Also investigated are some of the anticipated behaviors and requirements of supersonic aircraft in the commercial airspace.

I. Introduction

SUPERSONIC Technology Concept Aeroplanes† are conceptual research vehicles studied with the intent to provide information to the International Civil Aviation Organization by way of their Committee on Aviation Environmental Protection (CAEP). Though several STCAs are being investigated by CAEP, the focus of this paper is an analysis of an eight-passenger, Mach 1.4 business jet developed by NASA. The airplane is intended to be generally representative of early market entrant supersonic business jet aircraft being considered by industry. It is designed to travel transatlantic distances at Mach 1.4 using relatively near-term technologies. It is equipped with conceptual engines designed and assessed by NASA. They are derived from the core of a contemporary, "off-the-shelf" subsonic turbofan. All aspects of the airplane and engine have been developed entirely with information from the public domain. Being nonproprietary and transparent, the STCA is ideal for use in ICAO's public studies. NASA began work on the STCA in 2017 in support of ICAO. Since then, the STCA continues to serve as a notional reference airplane used in studies conducted by NASA [1-3] and by others [4-11]. Aircraft mission performance, airport-vicinity noise, and exhaust emissions are predicted for the STCA using NASA tools.

There are three motivations for this study. First, during the eleventh triennial cycle of CAEP, two subgroups were formed in 2016 by the rapporteurs of CAEP's noise and exhaust emissions working groups. The charter of these subgroups is to examine the suitability of existing noise and exhaust emission certification standards for new supersonic civil airplane types. The subgroups are tasked with developing appropriate standards and recommended practices to support anticipated entries of new supersonic civil transports. The ultimate goal of both subgroups is to recommend amendments to Part II, Chapter 12 of [12] and to Part III, Chapter 3 of [13] that more properly address noise and exhaust emissions of supersonic airplane types, respectively. Both subgroups are dedicated to ensuring that new supersonic transports operate responsibly in an environmentally sustainable manner. NASA is assisting these subgroups by acting as analysts and independent arbitrators and by providing unbiased, open assessments of supersonic civil aircraft.

Second, the Federal Aviation Administration Reauthorization Act of 2018 [14] requires the FAA to "exercise leadership in the creation of Federal and international policies, regulations, and standards relating to the certification and safe and efficient operation of civil supersonic aircraft." To this end, the FAA issued a notice of proposed rulemaking regarding landing and takeoff noise standards for supersonic aircraft in April, 2020 [15]. The FAA's intention is to revise its noise standards [16] to include provisions for future supersonic transports. NASA assisted the FAA in this effort.

*Aerospace Engineer, Propulsion Systems Analysis Branch, senior member AIAA.
†In referring to STCAs, "aeroplane" is the spelling used by ICAO. The spelling "airplane," however, is used in this paper.

Third, at CAEP's eleventh triennial meeting in 2019, the committee agreed to conduct an exploratory study on the global impact of future civil supersonic aircraft [17]. The FAA endorsed the study [18] and requested that NASA assist it by providing the STCA's performance, fuel burn, noise, and exhaust emission data. The CAEP study predicted the outcome of adding supersonic transports to the existing civil aircraft fleet. The study was part of CAEP's twelfth (previous) program cycle and has since been completed. The STCA was an analytical proxy for future supersonic business jet types. The influence that supersonic airplanes are expected to have on operations, fuel consumption, airport noise, and air quality were assessed. Aircraft noise and performance data for the STCA were required to support the exploratory study. Derivation of the data is documented in this paper. A public report of the exploratory study is expected by the 2022 meeting of the CAEP Steering Group.

Presented in this paper is a description of the STCA's propulsion and airframe analysis, operational noise abatement departure procedures, stage length performance, and noise-power-distance data. Also investigated are some of the anticipated behaviors and requirements of these aircraft in the commercial airspace. A revised assessment of the STCA's noise levels in a certification setting is described in a companion paper [19].

II. Airframe and Engines

Prerequisites for computing aircraft noise and performance (ANP) data are working multidisciplinary models for the vehicle. Airframe, weight, aerodynamics, and propulsion analyses taken from [2] are described in the following sections.

A. Concept Airframe

The STCA is a notional, eight-passenger business jet designed for Mach 1.4 supersonic overwater cruise speeds. It has a low-aspect ratio cranked delta wing. Three engines are mounted aft; the outboard engines are mounted on short fuselage pylons, while the center engine is integrated with the vertical tail. A summary of vehicle characteristics is shown in Table 1. A solid model of the airplane is shown in Figure 1 (half of the top view is drawn to show the interior arrangement and locations of fuel).

The airplane has no features that would reduce its sonic boom noise signature, making it similar in that respect to other early market entrant designs. Supersonic speeds over land would be restricted where prohibited. Despite NASA's current interest in low-boom supersonic aircraft [20], those types of designs are viewed here as candidates for later markets.

Table 1: STCA characteristics.

Max takeoff weight, klb	121
Passengers	8
Cruise Mach	1.4
Overall length, ft	135
Span, ft	67
Wing reference area, ft^2	1619
Wing aspect ratio	2.7
Wing taper ratio	0.09
Wing loading, lb/ft^2	74
Wing fuel, klb	24
Fuselage fuel, klb	36
Fuel fraction	0.50

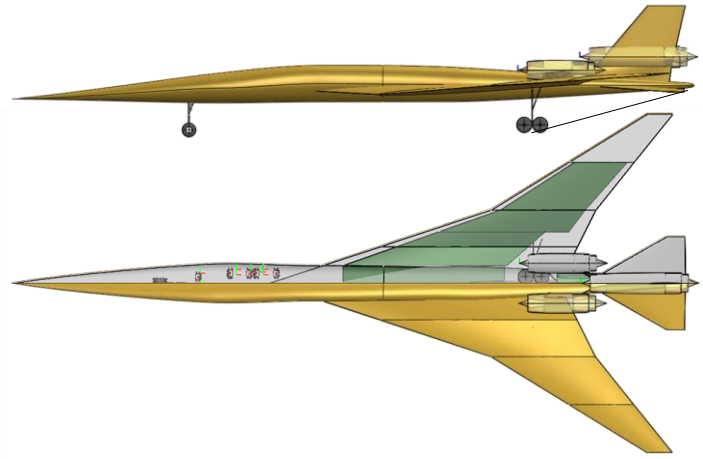

Figure 1. Solid model of the STCA.

Several aircraft conceptual design tools are used to synthesize the vehicle. A solid modeling tool [21] is used to define the outer mold lines of the airplane, to guide interior packaging, and to estimate internal fuel volume. The solid model also informs component weight and vehicle aerodynamic analyses. Lift-dependent drags, lift-independent drags, and wave drags are calculated by the methods described in Refs. [22-24]. A weight estimate of the wing is made using physics-based factors based on its gross geometry, while weight estimates of other major structures and systems are made using statistical-empirical relations. All airframe weight estimation methods are discussed in [25]. These computer codes are organized together using a frameworking tool [26] which provides a conceptual-level, multidisciplinary, integrated process for designing and analyzing supersonic aircraft [27]. Using this integrated design

environment, major aircraft design variables can be rapidly assessed and optimized. A design and sizing analysis of wing, fuselage and tail characteristics is performed, subject to practical performance constraints.

The vehicle design is optimized to maximize range for a fixed maximum gross weight of 55t (121klb). Subject to a minimum cabin width of 7ft, fuselage section height, width, and tangent angles at three stations are optimized to minimize wave drag. Wing planform shape, airfoil twist, and camber are varied to minimize wave drag and lift-dependent drag. Horizontal tail size and location, main gear location, and trailing edge and leading edge flap deflections are optimized to meet takeoff, landing, and cruise static margin constraints, and to ensure reasonable takeoff and landing field lengths and approach velocity.

B. Propulsion

For an early market entrant, it is unlikely that a completely new engine could be developed and be ready in time for a near-term entry into service. Instead, it is more likely that the low-pressure spool of a contemporary off-the-shelf engine would be redesigned and repurposed, resulting in a supersonic variant of an existing subsonic turbofan. In this study, an analytical model of a subsonic CFM International CFM56-7B27 is used as the "donor" engine from which the supersonic engine is derived. Interestingly, the original CFM56-2, granted certification in 1979, was itself derived from the General Electric F101 model used for the supersonic B-1A bomber. Redesigning the low-pressure spool of a CFM56 once again for a supersonic application would bring the engine family full circle.

Because much engine design data are closely-held, proprietary, and unavailable, any analytic simulation of a CFM56 (outside of CFM International) will necessarily have some inherent inaccuracy. Nevertheless, if data can be obtained from public-domain sources (such as type certificate data sheets, manufacturer-provided operating documents, technical reports, and manufacturer's websites), simulations of turbofans developed outside of engine companies can be reasonably accurate. A model of the subsonic CFM56 is created with such information using the Numerical Propulsion System Simulation code (NPSS, [28, 29]) to predict engine performance. NPSS is an engine cycle analysis tool developed jointly by NASA and by United States aerospace industry. It is currently the accepted, state-of-the-art software for airbreathing engine cycle performance analysis for United States industry, academia, and NASA. The subsonic CFM56 model is adapted from work performed under the FAA's Environmental Design Space initiative [30, 31].

The low-pressure spool of the CFM56-7B is redesigned for a Mach 1.4 cruise application. The booster is discarded (with it, supersonic ram effects would elevate aft stages of the compressor to excessive temperature), and the fan and low-pressure turbine are redesigned for a higher pressure ratio. Fan performance is modeled using data collected at NASA from the GE57 scale model fan [32]. The GE57 fan is considered to be perhaps representative of what might be used by an engine manufacturer in a supersonic refan application. It consists of a single stage and operates at peak efficiency at a pressure ratio of 2.2. Fan pressure ratio is a design variable strongly influencing engine performance. A high fan pressure ratio is preferred to create an exhaust velocity high enough for supersonic flight, while a low fan pressure ratio is required to meet takeoff and landing noise requirements. Fan pressure ratio, along with a practical extraction ratio, directly determine the bypass ratio of the engine. This poses conflicting requirements for supersonic engine designers. If fan pressure ratios are high enough, they could lead to supercritical nozzle pressure ratios at low altitude and create high levels of jet shock cell noise during takeoff.

Another design choice is whether to forcibly mix the core and bypass streams or to allow them to remain separate. There are compelling reasons to mix the streams. There is usually an increase in gross thrust when flows are forcibly mixed and exhausted through a common nozzle, with the benefit increasing with increasing core stream temperature. And the outer mold lines of a simpler, single-stream nozzle are preferred over those of a more complex coannular nozzle if sonic boom reduction is important. In this study, core and bypass streams are forcibly mixed through a lobed mixer. The design extraction ratio is kept near unity so that mixer bypass port and mixer exit Mach numbers are always less than 0.5.

The mixed flow exits through a single-stream convergent-divergent plug nozzle. The centerbody plug and nozzle throat are fixed while the divergent flaps are variable. The plug is important in keeping aftbody boattail angles small during supersonic cruise while also lowering takeoff jet noise slightly. At low altitudes, the divergent nozzle flaps are closed to a minimum area so that the nozzle exit plane is the throat. Solid models of the CFM56-7B and the derived supersonic variant are shown in Figure 2. Not shown in the figure are the nozzles or inlets for either engine.

At the cycle design point, characteristics of the compressor and the high-pressure turbine are set manually to those of the CFM56 donor engine. This keeps the high-pressure spool of the supersonic derivative engine identical to the CFM56 core. Bleed flow fractions and core flow passage areas are also held constant. Hot section temperatures are kept nearly as high as the CFM56 maximum takeoff temperatures. But since the supersonic variant would spend several hours at maximum temperature (compared to just a few minutes during takeoff for a subsonic turbofan), this becomes a rather important assumption. Maintaining high temperatures is justified by assuming increased hot section overhaul frequency (not uncommon for a business jet application), and perhaps by offering new turbine airfoils with improved materials, coatings, and better cooling effectiveness.

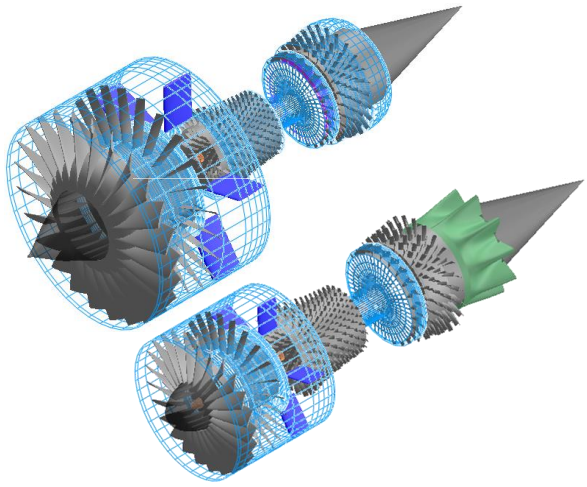

Figure 2. Solid models of the CFM56-7B (top) and conceptual modified supersonic variant (bottom).

Table 2. Performance summary for the STCA derivative engine.

	M1.4, 50kft, ISA	M0.25, sea level, ISA+27°F	Sea level static, ISA+27°F
Net thrust, lb/engine	3330	14,140	16,620
Specific fuel consumption, lb/hr/lb	0.943	0.588	0.479
Bypass ratio	2.9	2.9	3.0
Burner temperature, °R	3300	3150	3130
Turbine inlet temperature, °R	3180	3040	3020
Compressor exit temperature, °R	1450	1440	1430
Overall pressure ratio	22	21	21
Fan pressure ratio	2.0	1.9	1.9
Compressor pressure ratio	11.2	11.1	11.2
Extraction ratio	1.1	1.1	1.1
Nozzle pressure ratio	5.9	1.9	1.8

Fan pressure ratios are selected such that the nozzle operates on the cusp of choke near sea level. With a small amount of engine derating at low altitude, jet shock cell noise is eliminated during takeoff. A summary of engine performance data is shown in Table 2. Ambient conditions above 10,000 feet use International Standard Atmosphere (ISA) conditions, while conditions nearer sea level use hot day (ISA+27°F) conditions. Performance data at sea level are shown after engine derating.

Though the supersonic engine variant may appear similar to GE Aviation's Affinity™ engine [33] proposed for Aerion Supersonic's supersonic business jet, it is based on a NASA model predating Aerion Corporation's public partnership announcement with GE Aviation in 2018. It uses no company-proprietary information. Additional information for the STCA equipped with these engines is available in [2].

C. Mission performance

With aerodynamics, engine thrust and fuel consumption performance known, a mission analysis of the transport can be made using NASA mission performance software [34]. The design mission is at maximum takeoff gross weight, non-stop, with a single cruise segment at supersonic speed. There are no subsonic cruise segments which might be typical of other missions where supersonic flight might be restricted. Since high-altitude air traffic should be light, block altitude clearance is assumed and the airplane is allowed to climb continuously during supersonic cruise. The design mission uses the full payload complement of eight passengers. The mission rules described in [35] are followed, except that the five percent block fuel reserve allowance is omitted, which is more typical of mission rules followed by business jets. The mission profile is shown in Figure 3. The design mission range of the STCA is 4243nmi. Performance results for the STCA using the derivative engine are shown in Table 3.

Table 3: STCA performance.

Takeoff gross wt, klb	121
Operating empty wt, klb	51
Payload, lb	1640
Climb time, min	47
Cruise altitude, kft	44-51
Cruise lift-drag ratio	6.6-7.9
Block time, hr	5.9
Block fuel, klb	61
Reserve fuel, klb	8
Range, nmi	4243

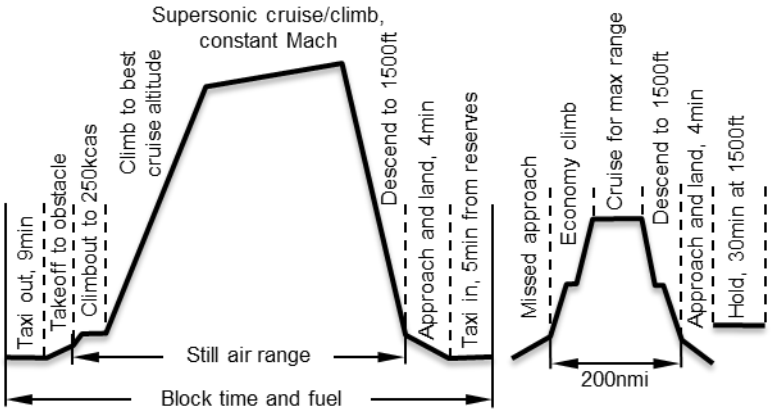

Figure 3. STCA mission profile.

III. Noise Prediction Method

Another prerequisite for computing ANP data for the vehicle is an acoustic model. In general, aircraft system noise prediction tools fall into one of two categories. Both categories are discussed here.

The first category of tools rely on so-called noise-power-distance (NPD) data as the basis for computing noise on the ground. This approach was originally proposed by SAE [36], revised [37], and most recently documented by ICAO [38]. Original equipment manufacturers of civil aircraft supply NPD data for their products so that their noise impact may be modeled. Manufacturers measure NPD data directly, scale or infer them from other NPD data, or predict them from first principles using computational tools in a scenario appropriate for measuring them. System noise codes based on NPD input data are said to be "ICAO Doc. 9911-compliant" in accordance with [38]. Examples are the Aviation Environmental Design Tool (AEDT) [39, 40] and others [41-44]. These tools, in a sense, start with the answer, because rudimentary noise characteristics for each airplane are given as tabular lookup data.

Other noise prediction codes, however, are less empirical and are based more on physics. They are more reliant on first principles, where lossless free-field spectra in the vicinity of an airplane are predicted and then propagated in a straight line to a receiver. Examples are NASA's Aircraft Noise Prediction Program (ANOPP, [45, 46]) and others [47-50]. The distinction between the two categories can blur, however, since codes like ANOPP can be coaxed into generating NPD data for use in Doc. 9911-compliant tools.

All noise predictions for the STCA (including its NPD data) are made using NASA's ANOPP, with predictive methods selected to represent the noise sources of a supersonic business jet. It should be noted that applying empirical methods that were developed largely for conventional subsonic transports (powered by high bypass ratio, separate-flow turbofans) to a supersonic delta-wing airplane (equipped with low bypass ratio engines with supersonic inlets, long-duct mixers, and more complex nozzles) has a high uncertainty. Sensitivities to uncertainty are assessed in the previous study [2].

Jet noise is predicted using an empirical method developed by the Society of Automotive Engineers [51]. For simple, single-stream, round nozzles operating on the cusp of choke, the SAE method is preferred over other available methods based on comparisons of predicted levels to scale model and flight test data [52, 53]. Since jet noise is typically the dominant source in supersonic applications, it is the subject of recent studies at NASA [54-57].

Broadband fan noise is predicted using an empirical method developed by General Electric [58], and discrete fan interaction tones are predicted using a similar method [59] (both of these methods are more recent calibrations of ANOPP's original fan noise method). For predicting noise of high-speed, high-pressure-ratio, single-stage fans that might be used in a supersonic application, these methods are preferred based on comparisons made to data collected by NASA: the General Electric High Speed Fan [60], the Honeywell Quiet High Speed Fan [61], and a two-stage fan designed and built by Pratt & Whitney as part of the NASA-led High Speed Research Program. Fan treatment suppression is estimated using a method developed by General Electric [62].

Engine core noise is predicted by a method developed by Emmerling [63]. Engine state data computed by NPSS are fed into ANOPP as functions of flight speed, altitude, and engine power setting.

Landing gear, flap, slat and trailing edge airframe sources are predicted using a recalibrated version of the empirical Fink method [64]. The recalibrated model is based on noise measurements of a supersonic delta-wing transport [65]

and is documented in [66]. The predicted levels are adjusted to represent airframe noise levels of a notional supersonic business jet.

With engines mounted above the vehicle, noise shielding effects must be considered. Shielding (also referred to as barrier attenuation or insertion loss) is an acoustic diffraction phenomenon where sound waves are attenuated when propagated past an impermeable barrier placed between the noise source and an observer. In this study, a simple empirical diffraction model based on optical diffraction theory is used. The model was originally proposed by Maekawa [67] and is reproduced in many foundational acoustic textbooks. Shielding is particularly efficient when the observer is located in the "shadow region" where the noise source is obscured. The delta wing (see Figure 1) provides excellent shielding of forward-radiated fan inlet noise. All other sources are not shielded. Jet noise is a distributed source generated downstream throughout the axial exhaust plume. Core noise is predominantly aft-radiating and is assumed to radiate through the exhaust. Fan exit noise also escapes through the nozzle but it is attenuated by treatment in the bypass duct.

Noise levels of all components are predicted as lossless, one-third octave band spectra and are summed in the vicinity of the airplane. The noise sources are predicted at various flight conditions (i.e., the NPD "evaluation points" described in the next section). The noise levels are propagated to a pole-mounted receiver located on the ground. NPD data are computed as explained in Section VI. Noise propagation effects include spherical spreading, Doppler shift and convective amplification, atmospheric absorption, and ground reflections [68] based on data for grass-covered ground [69]. The atmospheric absorption model required for NPD data [37] differs from the absorption model used for noise certification [70].

IV. Noise Abatement Departure Procedures

ICAO Doc. 9911-compliant codes require a flight track to be defined in the terminal airspace for every airplane operation so that noise contours on the ground can be computed. Flight tracks may be defined either by fixed-point profiles or by procedural step calculations using simplified equations of motion and airplane performance data. Flight tracks for the STCA are defined using the fixed-point profile option. The profile data consist of points defined in space and time (viz. airspeed), and by aircraft configuration and engine power setting. Both departure and arrival profiles are computed.

The state of the engine, the airplane and its flight track have first-order influences on airport-vicinity noise. For Doc. 9911-compliant codes to predict operational noise most accurately, the flight tracks should be consistent with those used in real-world operations. Noise Abatement Departure Procedures (NADPs; sometimes referred to as Noise Abatement Departure Profiles) are popular in modern civil aviation, and an airplane such as the STCA would be likely to use them. This section provides an overview of NADPs for the STCA.

Operational NADPs differ from takeoff procedures used in noise certification. Reference procedures of Annex 16 noise regulations [12] are generally more restrictive than procedures ordinarily found in operational practice. For example, noise certification reference procedures described in Section 3.6.2(d) of the Annex require a constant climbout speed, whereas NADPs typically include at least one in-air acceleration segment. And in practice, pilot-initiated engine power cutbacks differ from those permitted in Section 3.6.2(b). In noise certification, power cutbacks are usually much deeper.

There are other differences as well, including two that might be unique to supersonic transports (though at this writing, applicability to subsonic transports is under discussion). The first pertains to engine thrust management. Section 3.6.2(a) of the Annex requires that takeoff thrust be maintained from brake release until the point where the pilot-initiated thrust cutback is permitted. However, a programmed lapse rate (PLR) procedure is under discussion among regulators for future supersonic aircraft [15]. The PLR procedure is a thrust lapse programmed to occur automatically at low altitudes. It is not to be confused with the *pilot-initiated* engine power cutback occurring later. It would be employed both during noise certification and in normal operations. In certification, a PLR procedure would reduce noise at the lateral certification monitor, and in operation it would reduce noise near airports. A more detailed discussion of PLR procedures and how one is envisioned to be implemented for the STCA can be found in Refs. [2] and [19].

The second difference pertains to airframe configuration changes. Section 3.6.2(e) of the Annex requires the position of high-lift devices be maintained throughout the reference procedure. This differs from operational practice, where flaps and slats are retracted on sensible schedules. In a manner similar to the PLR procedure, it should be possible to program flaps to retract automatically.

Both of these procedures could be implemented as a Variable Noise Reduction System (VNRS) under the provisions of [71]. Normally, regulating authorities might be reluctant to approve any pilot-initiated procedure that would increase the workload of the flight crew at low altitudes. But it is thought that exceptions would be permitted

if computer-controlled automatic throttle scheduling and flap retraction are used, making pilot initiation unnecessary. An automatic digital engine control implementation of these procedures could use an airplane's weight-on-wheels sensors, airspeed, altimeter, attitude and air temperature indicators, or perhaps airport navigational aids to begin preprogrammed actions. A companion paper describing the use of a VNRS to minimize noise of the STCA in a certification scenario has been written [19].

The methods and tools used to derive departure profile data for the STCA are selected by NASA. Derivation of data for other aircraft are likely to use other methods, tools, and selection criteria. This paper documents NASA's approach.

A. NADP Characteristics

ICAO [72] and FAA [73] recommend NADPs for operators of turbine-engine airplanes over 75,000lb. Procedures must be consistent with existing airworthiness standards. No more than two procedures for each aircraft type are recommended.

Profiles having a close-in noise benefit are intended to abate noise for communities close to airports. These profiles are often characterized by an early pilot-initiated engine power cutback and an initial climb at constant airspeed with takeoff flaps deployed. From that point, the profiles continue typically with a flap retraction and an acceleration segment. These procedures are named NADP-1, close-in NADP, or ICAO-A. The latter name is used in AEDT, though the terminology is now obsolete.

Alternately, profiles having a distant noise benefit are intended to abate noise for communities far from airports. These profiles are usually characterized by an early flap retraction and an acceleration segment. These procedures are named NADP-2, distant NADP, or ICAO-B (now obsolete).

In general, close-in procedures tend to devote more of the vehicle's total available energy towards increasing its potential energy (i.e., altitude) than distant procedures do. A generalized schematic of noise abatement departure procedures is shown in Figure 4.

Note that the PLR procedure is indicated on the figure. A discussion of the PLR procedure as implemented by NASA for the STCA is can be found in [2]. The STCA is assumed to have completed its PLR procedure before specific NADP steps begin. The goal of this study is to select one close-in benefit profile (in the style of NADP-1) and one distant benefit profile (in the style of NADP-2) for the STCA.

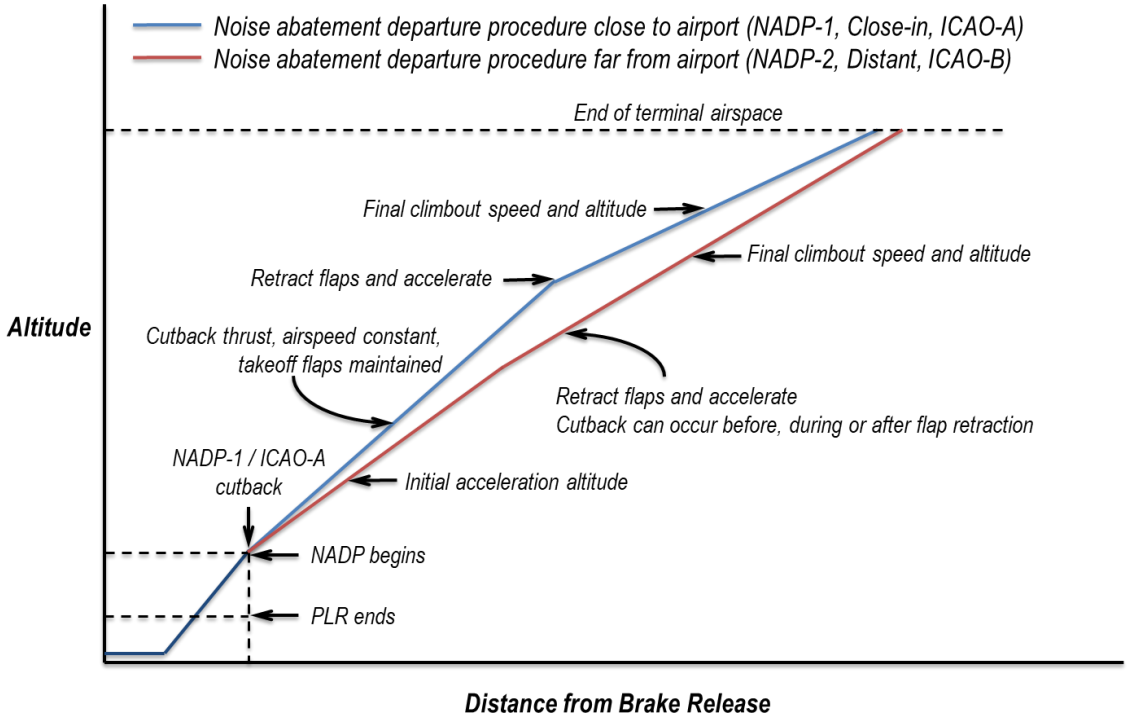

Figure 4. NADP schematics.

B. Survey of the Aircraft Noise and Performance Database

Most of the details of NADPs are unspecified and are left to manufacturers to determine. Accelerations, changes in configuration, engine power and the sequence and timing of events are not always consistent from manufacturer to manufacturer, or even from product to product. With so many variables involved, it is not immediately obvious how the STCA should be flown. Therefore, a survey of the Aircraft Noise and Performance database (defined in a Doc. 9911 appendix and available online [74]) is used to guide the selection of profile parameters for the STCA's operational profiles. Nomenclature in this survey corresponds to that used in AEDT. Departure procedures considered are ICAO-A, ICAO-B, and DEFAULT (also known as STANDARD). Some aircraft types are omitted from the survey.

Each departure procedure in the ANP database is examined for its cutback trigger (i.e., the criterion that determines when engine power is reduced), cutback level (the reduced engine power setting), flap retraction trigger (the criterion for flap retraction), acceleration trigger (the criterion for one or more acceleration segments), and airspeeds. Note that any ICAO-A, ICAO-B, or DEFAULT procedure in the ANP database can be classified as either a close-in noise benefit or a distant noise benefit. From the survey, the following observations are made:

1. ICAO-A and NADP-1 procedures are identical.
2. ICAO-B and NADP-2 procedures are nearly identical, except that:
    - ICAO-B cutbacks occur after the acceleration segment.
    - NADP-2 cutbacks occur "during the flap/slat retraction sequence at a point that ensures satisfactory acceleration performance" [72].
3. DEFAULT procedures can be classified as either close-in or distant (but nearly all of them are distant).
4. In modern operational practice, "distant benefit" departures are commonly flown as NADP-2 [75].
5. Aérospatiale/BAC Concorde exits the terminal airspace (i.e., 10,000ft above field elevation) at 250kcas.
6. 10 airplane types exit the terminal airspace at speeds above 250kcas.
7. One 747 type exits the terminal airspace at 300kcas.

The latter three items are relevant for supersonic transports, which typically have a preference for high airspeed at low altitudes. These observations are important in setting NADPs for the STCA, as discussed in the following section.

C. Parametric Variation and Selection of Departure Variables

A flowchart describing how the STCA may be flown using different procedures is adapted from [75] and is shown in Figure 5. Major independent variables are parameterized; these are labeled using the letters "A" through "N" in the flowchart. Rather than allow the independent variables to be continuous-real, they are assigned discrete values with the intent to perform an optimization based on a factorial design of experiments. This type of grid-based optimization is an "exhaustive search." The cost of this brute-force strategy is higher than a search aided by an optimizer. But if each objective sample runs reasonably fast, it is attractive since finding the global optimum is virtually ensured (provided the grid intervals are sufficiently fine). The optimal NADP designs are selected simply by inspection. The danger of an optimizer becoming "stuck" on a local optimum is thus avoided. The left side of the flowchart is intended to represent departure procedures patterned after NADP-1/ICAO-A; while the right side represents procedures are patterned after NADP-2/ICAO-B. The independent variables are permuted using discrete values shown in the figure, and each resulting NADP profile is examined for merit as explained below.

For the STCA, all NADP procedures begin at 400ft above field elevation. This is at the beginning of the second climb segment when the airplane has reached its takeoff safety speed plus 35kt (i.e., V_2+35kt, as explained in [2]). By that altitude, it has completed its programmed thrust lapse and its gear has been fully retracted. All takeoff profiles are evaluated at maximum gross weight from a sea level field.

Three pilot-initiated engine power cutback levels are investigated (see Figure 5). The range is defined by the thrusts required to maintain climb gradients of 1.5, 2.0, and 2.5% with one engine inoperative (note that 1.5% is the minimum climb gradient from 400ft to 1500ft permitted for trijets per §25.111 of [76]).

Two terminal airspeeds are investigated (these are airspeeds achieved upon exiting the terminal airspace at 10,000ft above field elevation). Referring to Figure 5, the exit airspeeds for the STCA are either 250kcas or 290kcas. 250kcas is a logical choice because, unless otherwise authorized, it is the maximum airspeed allowed under 10,000ft in the U.S. per §91.117 of [77]. Other countries have also adopted this speed limit. Thus, exiting the terminal airspace at the 290kcas higher speed requires some justification.

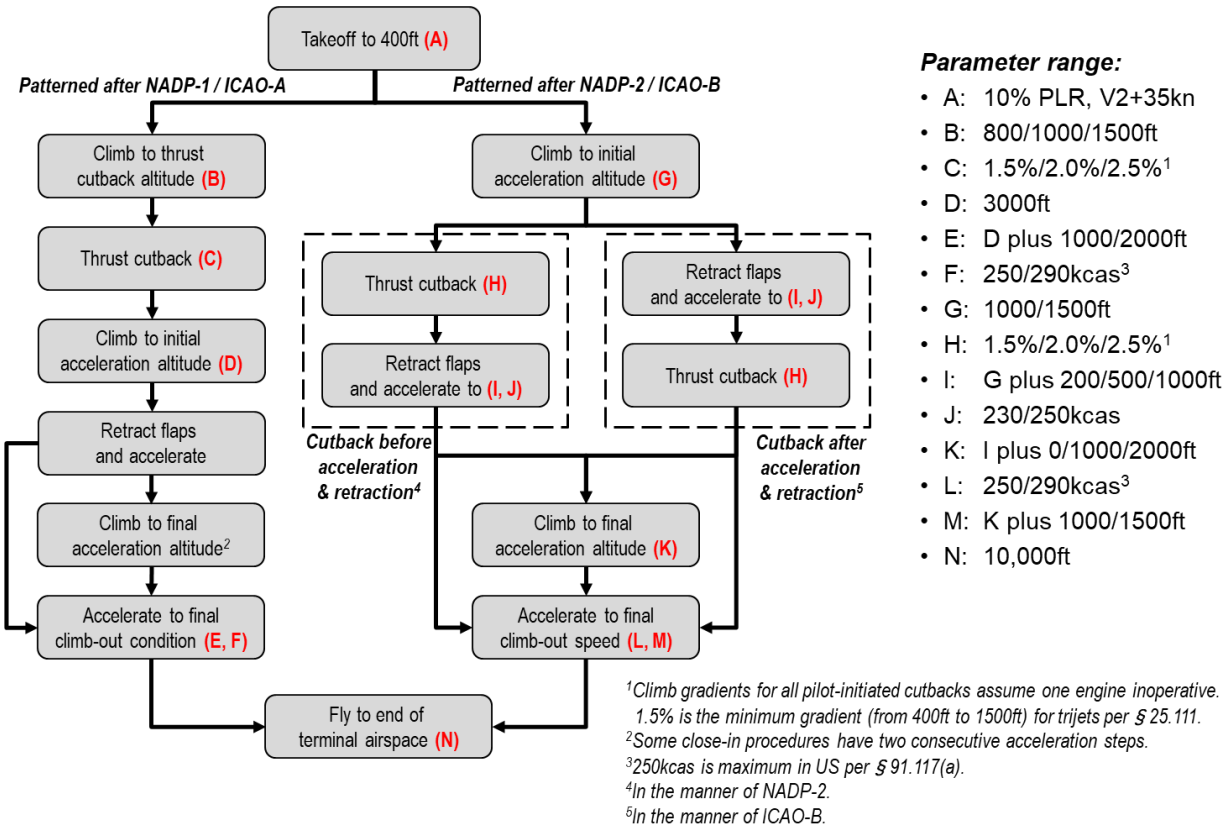

Figure 5. Flowchart formulation and parametrization of variables.

Higher exit speeds are found in the ANP database survey, as discussed in the section above. And the STCA, like many supersonic airplanes, has a preference for high airspeeds at low altitudes. A chart showing the STCA's thrust demand is shown in Figure 6 for level and steady flight at maximum weight at an altitude of 2000 feet. Noted in the figure is the takeoff safety speed (V_2), determined by a one-engine inoperative, balanced field calculation following the guidance in [76], and the 250kcas speed limit. The STCA's minimum drag speed is nearly 280kcas. Speeds below this are in the so-called region of reversed command, where to fly more slowly requires more thrust to overcome increasing lift-dependent drag. This is in contrast to a similarly-sized subsonic airplane with takeoff flap deflections in these conditions, which may have a minimum drag speed of perhaps only 200kcas. Flying safely in this region requires adequate thrust margins, shown in the figure as the difference between available thrust and required thrust with all engines operating and with one engine inoperative. Supersonic transports are likely to have thin wings with low aspect ratios and simple flap systems. They are likely to require high takeoff speeds before sufficient lift is generated to lift off, and even higher airspeeds to climb with significant thrust margin. In contrast with most subsonic transports, in-air acceleration segments to high airspeeds are preferred for supersonic transports. In operational practice, it was common for the Concorde to accelerate and to reach 250kcas by 400ft above field elevation [74], and similar in-air accelerations were planned for the proposed supersonic High-Speed Civil Transport [78, 79]. In this study, 290kcas is justified since it is close to the STCA's minimum drag speed.

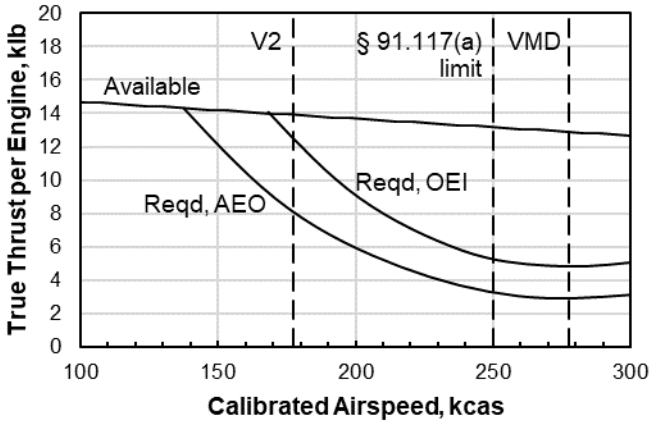

Figure 6. Thrust demand of the STCA in level, steady flight.

With the parameterization of departure variables chosen (see Figure 5), 48 and 216 possible combinations are identified for NADP-1 and NADP-2 profiles, respectively. Each of these profiles is analytically "flown" using a forward-differencing trajectory solver that satisfies the equations of motion at discrete intervals [80]. Using the noise methods described in Section III, the sound exposure level (SEL) noise metric is evaluated for ground observers located directly under the flight path of each trajectory. A new noise metric is created to determine the merit of each profile. The metric consists of the area under the curve of SEL and distance from the airport (in units of dBA-nmi). The curve is weighted to emphasize SELs close to the airport, or far from the airport, depending on whether NADP-1 or NADP-2 profiles are assessed. Additional preference is given to profiles exiting the terminal airspace at 290kcas. The best profiles are chosen by inspection. The preferred NADP-1 and NADP-2 profiles for the STCA are shown in Figure 7. For comparison purposes, the Annex 16 noise certification profile computed in [2] is also shown. Also shown in the figure are "evaluation points" for computing noise-power-distance (NPD) data. They are roughly representative of the flight conditions for any departure procedure. These NPD evaluation points will be discussed further in Section VI.

V. Influence of Stage Length on NADPs

The NADPs determined for the STCA in the previous section are evaluated at maximum takeoff gross weight. But of course in operational practice, airplanes do not always depart at maximum gross weight. And since gross weight influences an airplane's takeoff trajectory, additional NADP profiles at gross weights less than maximum are required. The logic to determine these weights and the takeoff profiles associated with them are discussed in this section.

When making noise evaluations, AEDT models operations between airport pairs according to trip distance intervals. For simplicity, operations are cast into discrete bins called stage lengths. When a code such as AEDT is used to perform a multiple-event fleet noise analysis, a stage length must be assigned to each operation. Stage lengths consist of representative trip distances and the corresponding takeoff gross weights needed to fly those distances. Stage length is a surrogate indicator of takeoff gross weight. Using the same departure procedures defined in the previous section, additional profiles must be developed for the stage length missions at lower gross weights. Stage lengths defined for the STCA are shown in Table 4. A takeoff gross weight is sought for each stage length so that additional NADPs can be computed for them.

To determine the weight and fuel required for each stage length, an optimized mission planning calculation is required. Mission range performance is a strong function of fuel load, takeoff gross weight, and how the mission is flown. Cruise variables for the STCA are selected that optimize each mission. Logically, the optimization variable for a supersonic business jet like the STCA is block time. However, depending on the distance flown, additional considerations are given for block fuel, climb time, and practicality.

The following mission constraints are assumed. Breguet climbing cruise is assumed at altitudes over 40,000ft, where block altitude clearance is expected. The crew is assumed to use on-board programmed guidance to manually achieve a climbing cruise, or perhaps it will be automatically programmed into airplane flight management computers. The maximum subsonic and supersonic Mach numbers

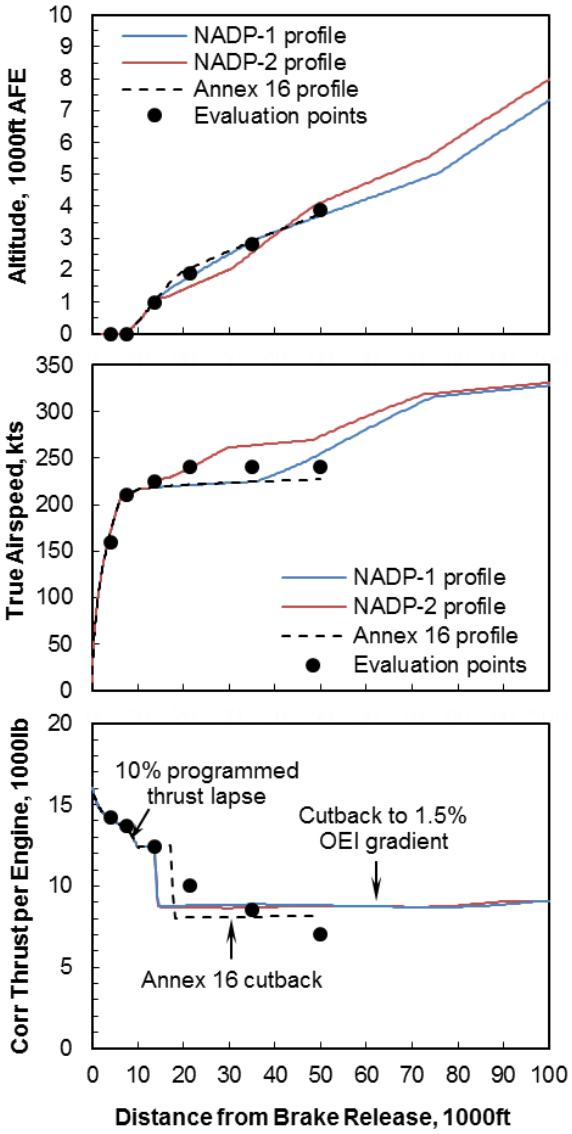

Figure 7. Departure profiles for the STCA.

allowed are 0.92 and 1.4, respectively. Fixed altitude cruise is assumed under 45,000ft. Supersonic speed is allowed only over 40,000ft. Cruise altitude and speed are optimized for each stage length, using a composite objective consisting of block time and block fuel. Results are discussed below.

1. Primary Stage Length Performance:

Supersonic airplanes like the STCA (with no features to reduce its sonic boom) are likely to have restrictions on supersonic overland flight. A realistic mission between a specific city pair might consist of multiple cruise segments and speeds to avoid flying at supersonic speeds where prohibited. Indeed, route planning for supersonic airplanes can become quite complicated [11, 81]. But to evaluate noise using a tool like AEDT, the stage lengths defined for each vehicle type are generic (i.e., there are no specific city pairs associated with any stage distance). For a subsonic airplane, this is not usually a concern. But for the STCA, stage length performance differs significantly when restrictions are placed on cruise speed. In this study, the modeling shortcomings are simply accepted. Mission assessments are made strictly on the basis of overall vehicle performance.

With no such restrictions, supersonic Breguet cruises at Mach 1.4 are preferred for the three longest stage lengths (2200, 3200, and 4240nmi). However, as trip distance becomes shorter, the block time metric shows diminishing returns and it becomes sensible to consider block fuel as an additional measure of merit. A subsonic cruise at Mach 0.92 is preferred for the three shortest stage lengths (350, 850, and 1350nmi). Since a supersonic business jet operator would presumably fly most often at supersonic speeds when appropriate, this stage performance is named primary stage performance. These are shown on the left side of Figure 8.

2. Alternate Subsonic Stage Length Performance:

Unlike subsonic airplanes, supersonic airplanes have multi-Mach cruise speed options. Even when flying over water with no restriction on speed, the operator of a supersonic airplane has the option of flying at subsonic speed. In the case of the STCA, its subsonic cruise range is substantially greater than its supersonic cruise range (note this may not be true of all supersonic aircraft). But given the option, it is possible that an operator might elect to save fuel or to fly further by cruising at a subsonic speed at the expense of time. Thus, alternate ranges are given for the STCA where all-subsonic missions are flown for the three longer stage lengths. Above 40,000ft, block altitude clearance is assumed and a Breguet cruise is allowed. Alternate subsonic stage length performance is shown on the right side of Figure 8. Performance for all stage lengths is shown in Table 4.

3. Departure Engine Power Management

At each gross weight, engine power management must be defined. Beginning with AEDT version 3b in 2019, the option of reduced thrust takeoffs became available (See Section 3.6.2.3 of the AEDT3b Technical Manual [39]). The reduced thrust setting models part-power takeoffs (that are common in practice) when maximum thrust is not required. However, this option was not used in the CAEP supersonic exploratory study. For the CAEP study, maximum takeoff thrust available was used from the beginning of the takeoff roll to the pilot-initiated cutback. Field lengths and climb performance were allowed to vary.

Table 4. STCA preferred stage lengths.

Stage number	Trip length (nmi)	Representative Range (nmi)	Weight, lb	Alternate Subsonic Range (nmi)
1	0-500	350	66000	-
2	500-1000	850	70500	-
3	1000-1500	1350	75200	-
4	1500-2500	2200	89600	3120
5	2500-3500	3200	104100	4450
M	Maximum range at MTOW	4240	121000	5820

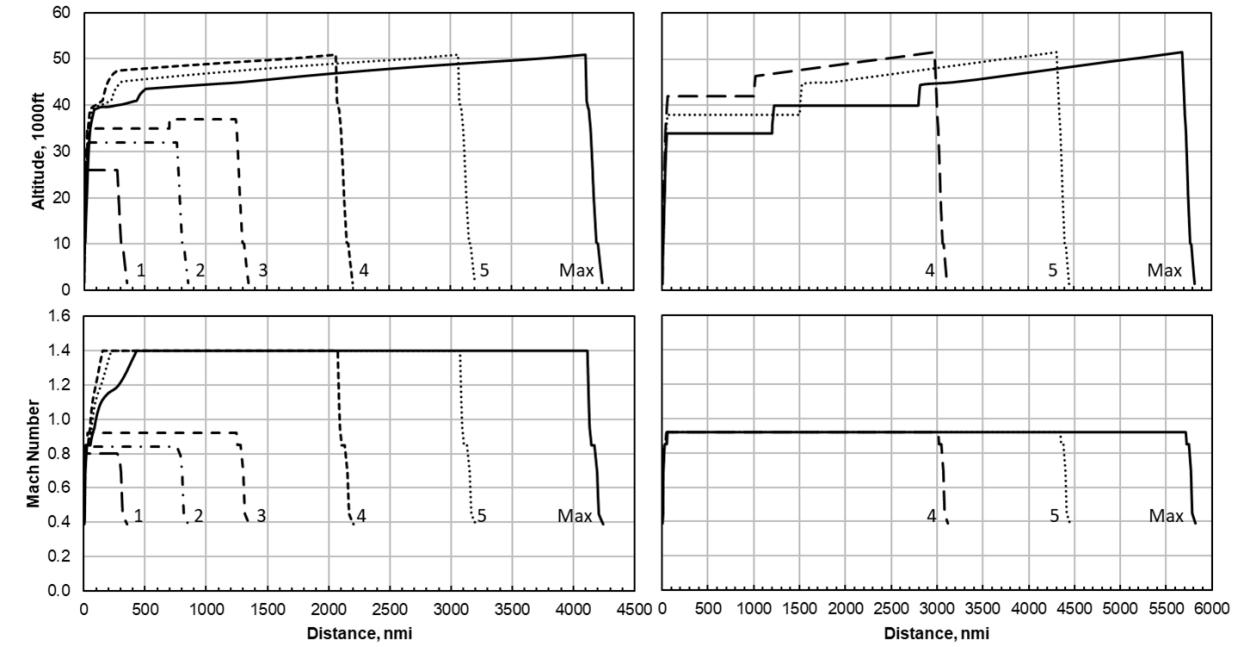

Figure 8. STCA primary stage length performance (left); alternate subsonic stage length performance (right).

VI. Noise-Power-Distance Data

ANOPP is used to predict all four types of NPD data used by AEDT: sound exposure level, maximum A-weighted level, maximum tone-corrected perceived noise level (PNLTmax), and effective perceived noise level (EPNL). And since ANOPP operates on the one-third octave band paradigm, all spectral data (computed natively by ANOPP) are also available for use in AEDT. The airplane is flown over an observer at altitudes ranging from 200ft to 25,000ft at ten discrete engine power settings. The simulated pole-mounted receiver is located 4ft above ground level. Ground reflection calculations are enabled. The atmospheric absorption model [37] required by AEDT is applied to the propagation calculations.

Noise sources are functions of airspeed and altitude. Jet noise, for example, is caused largely by turbulent mixing of the jet with ambient air. Strength of the shear layer is reduced as the airplane flies faster, and so jet noise is strongly influenced by airspeed. And naturally, airframe noise varies strongly with airspeed. Indeed, all sources are influenced by convective amplification and Doppler effects that vary with airspeed. So, in order to predict noise accurately for NADP profiles, noise predictions should be made at airspeeds that are most applicable to flight conditions of the NADPs. Thus, with the noise prediction methods described in Section III, and with the flight conditions determined for NADPs in Section IV, noise-power-distance data for the STCA can be calculated.

If NPD data are computed via ANOPP, appropriate airspeeds must be provided by the user for each value of corrected net thrust per engine. Since thrust is one of the independent variables of NPD data, the airspeeds should be values that are most appropriate for the thrust in question. For the STCA, these airspeeds are at the profile conditions labeled “evaluation points” in Figure 7. The NPD evaluation points are selected to be roughly representative of the flight conditions encountered during any departure procedure.

But the reference airspeed for NPD data in all Doc. 9911-compliant tools is 160ktas. In other words, whenever a compliant tool such as AEDT queries an NPD table, the noise metric returned is expected to be appropriate for a flight profile segment “flown” past a receiver at 160ktas. If the flight segment of the user-specified profile is at some other airspeed (and it usually is), AEDT makes an adjustment to the duration-dependent metrics SEL and EPNL. Therefore, before SEL and EPNL values computed by ANOPP can be ready for use in a code like AEDT, a “counter adjustment” must be made to them. This correction is a post-processing adjustment is added to the SEL and EPNL levels after they are computed by ANOPP (the adjustment is $10\log_{10}$[VTAS/160ktas], where VTAS is the true airspeed of the NPD evaluation point).

Adding more independent variables can increase the accuracy of NPD data. Multi-speed NPD data, for example, would include airspeed as an additional independent table lookup variable. This would ensure more accurate modeling of noise sources that are strong functions of airspeed, such as jet noise and airframe noise. The STCA, for example,

might benefit from additional NPD data above 250ktas (see Figure 7). Research is ongoing [75, 82] that may result in adding airspeed-dependent NPD data to future versions of AEDT.

Corrected net thrust levels are chosen to cover the range of engine operation expected in practice. The NPD data for the STCA are shown in Figure 9. They are ready for use in AEDT. The data were provided to CAEP analysts performing the supersonic exploratory study.

The STCA's NPD data (unadjusted for airspeed) can be used to check the Annex 16 certification noise levels made in a previous ANOPP simulation (see [2]). Table lookup errors for EPNL and PNLTmax for flyover and approach conditions are less than 1dB. These lookup errors are attributed to the following modeling differences between the NPD simulation and the Annex 16 certification noise simulation:

- Layered atmosphere at ISA+18°F (certification predictions) vs. a homogeneous atmosphere at ISA (NPD predictions).
- SAE ARP 866A absorption (certification predictions) vs. SAE AIR 1845A absorption (NPD predictions).
- More realistic profiles with variable engine thrust (certification predictions) vs. level, steady flyovers at constant engine thrust (NPD predictions).

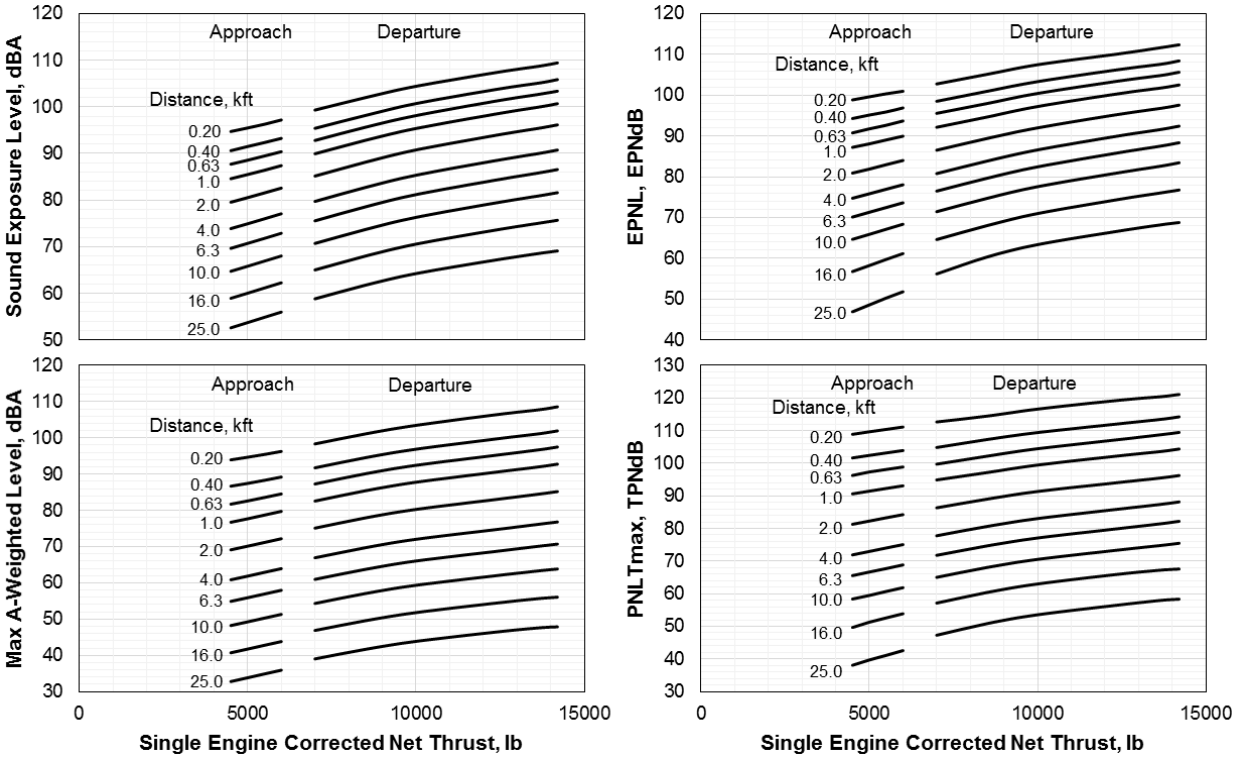

Figure 9. STCA noise-power-distance data.

VII. Summary

A notional 55-tonne supersonic technology concept airplane is discussed in this paper. It has been developed and studied by NASA at the request of the FAA and ICAO. The behavior of the STCA in an operational setting is considered. Aircraft noise and performance data consisting of noise abatement departure procedures, stage length performance, and noise-power-distance data are predicted. NASA tools are used to compute all data. Limitations are discussed in the paper. Also investigated are some of the anticipated behaviors and requirements of supersonic aircraft in the terminal airspace. The influence that future supersonic airplanes will have on operations, fuel consumption, airport noise, and air quality has been assessed by a CAEP supersonic exploratory study. The STCA served as an analytical proxy for similar early market entrant supersonic airplane types. Being nonproprietary and transparent, the STCA is ideal for use in ICAO's public studies. The data presented in this paper were provided to CAEP analysts for the study.

VIII. Acknowledgments

Thanks to NASA's Commercial Supersonic Technology Project for supporting this study. Thanks also go to the International Coordinating Council of Aerospace Industries Associations, particularly GE Aviation and Gulfstream Aerospace Corporation, for their helpful guidance and suggestions. Thanks go to ICAO's Working Group 1 (Aircraft Noise, Technical), and to the FAA, for including supersonic research into their work programs. Together, they are helping the world understand the impacts of future civil supersonic transports. The vision of viable supersonic transports operating responsibly in an environmentally sustainable manner is a shared pursuit.

References

[1] Berton, J. J.; Jones, S. M.; Seidel, J. A.; and Huff, D. L., "Noise predictions for a Supersonic Business Jet using Advanced Take-off Procedures," The Aeronautical Journal, Royal Aeronautical Society, Vol. 122 (1250), 2018, pp. 556-571 (doi: 10.1017/aer.2018.6).

[2] Berton, J.; Huff, D.; Seidel, J.; and Geiselhart, K.: "Supersonic Technology Concept Aeroplanes for Environmental Studies," AIAA Paper 2020-0263, AIAA SciTech Forum and Exposition, Orlando, FL, 6-10 Jan, 2020 (doi 10.2514/6.2020-0263).

[3] Rizzi, S.; Berton, J.; and Tuttle, B.: "Auralization of a Supersonic Business Jet Using Advanced Takeoff Procedures," AIAA Paper 2020-0266, AIAA SciTech Forum and Exposition, Orlando, FL, 6-10 Jan, 2020 (doi 10.2514/6.2020-0266).

[4] Nöding, M.; Schuermann, M.; Bertsch, L.; Koch, M.; Plohr, M.; Jaron, R.; and Berton, J.: "Simulation of Landing and Take-off Noise for Supersonic Transport Aircraft at a Conceptual Design Fidelity Level," *MDPI J. Aerospace*, vol. 9, no. 1, 2022 (doi 10.3390/aerospace9010009).

[5] Nöding, M.; and Bertsch, L.: "Application of Noise Certification Regulations within Conceptual Aircraft Design," *MDPI J. Aerospace*, vol. 8, no. 8, 2021 (doi 10.3390/aerospace8080210).

[6] Akatsuka, J.; and Ishii, T.: "System Noise Assessment of NASA Supersonic Technology Concept Aeroplane Using JAXA's Noise Prediction Tool," AIAA paper 2020-0265, 2020 (doi 10.2514/6.2020-0265).

[7] Akatsuka, J.; and Ishii, T.: "Comparative Study of Semi-empirical Jet Noise Prediction Models for Future Commercial Supersonic Aircraft," AIAA paper 2021-2219, 2021 (doi 10.2514/6.2021-2219).

[8] Rutherford, D.; Eastham, S.; Sanz-Morère, I.; Kim, J.; and Speth, R.: "Environmental limits on supersonic aircraft in 2035," International Council on Clean Transportation, Working Paper 2202-02, Jan. 2022 [URL: https://theicct.org/wp-content/uploads/2022/01/aviation-global-supersonic-safs-feb22-1.pdf, retrieved Feb. 2022].

[9] Barrett, S.: "Clean-Sheet Supersonic Aircraft Engine Design and Performance Annual Report," Aviation Sustainability Center (ASCENT) Project 47 Annual Report, Pullman, WA, 2020.

[10] Voet, L.; Prashanth, P.; Speth, R.; Sabnis, J.; Tan, C.; and Barrett, S.: "The impact of Design Space Constraints on the Noise and Emissions from Derivative Engines for Civil Supersonic Aircraft," AIAA paper 2021-1272, 2021 (doi 10.2514/6.2021-1272).

[11] Mavris, D.; Crossley, W.; Tai, J.; and DeLaurentis, D.: "Aircraft Technology Modeling and Assessment," Aviation Sustainability Center (ASCENT) Project 10 Annual Report, Pullman, WA, 2020.

[12] "Annex 16 to the Convention on International Civil Aviation, Vol. I: Aircraft Noise," *International Standards and Recommended Practices – Environmental Protection*, 7th ed., International Civil Aviation Organization, Montreal, July 2014.

[13] "Annex 16 to the Convention on International Civil Aviation, Vol. II: Aircraft Engine Emissions," *International Standards and Recommended Practices – Environmental Protection*, 3rd ed., International Civil Aviation Organization, Montreal, July 2008.

[14] U.S. Congress, "FAA Reauthorization Act of 2018, Section 181: FAA Leadership on Civil Supersonic Aircraft," 115th Congress, 2nd Session, H.R. 302, 3 Jan. 2018.

[15] Federal Aviation Administration, "Noise Certification of Supersonic Airplanes," Notice of Proposed Rulemaking, docket no. FAA-2020-0316, notice no. 20-06, 2020 [URL: https://www.federalregister.gov/documents/2020/04/13/2020-07039/noise-certification-of-supersonic-airplanes, retrieved December 2021].

[16] "Noise Standards: Aircraft Type and Airworthiness Certification," U.S. Code of Federal Regulations, Federal Aviation Advisory Circular 36-4C, 2003, Title 14, Chap. 1, Part 36.

[17] International Civil Aviation Organization: "Development of Supersonic Aeroplanes Subject to Public Acceptability Based on Subsonic Standards," Working Paper 103, Assembly (40th session), presented by Finland, 24 July 2019 [URL: https://www.icao.int/Meetings/a40/Documents/WP/wp_103_en.pdf, retrieved Dec. 2021].

[18] International Civil Aviation Organization: "Views of the United States on Civil Supersonic Flight," Working Paper 261, Assembly (40th session), presented by the United States, 2 Aug. 2019 [URL: https://www.icao.int/Meetings/A40/Documents /WP/wp_261_en.pdf, retrieved Dec. 2021].

[19] Berton, J.: "Variable Noise Reduction Systems for a Supersonic Technology Concept Aeroplane," AIAA Paper to be published, 28th AIAA/CEAS Aeroacoustics Conference, Southampton, UK, 14-17 June, 2022.

[20] National Aeronautics and Space Administration, "NASA Awards Contract to Build Quieter Supersonic Aircraft," Press release 18-20, April 2018.

[21] Gloudemans, J.; Davis, P.; and Gelhausen, P., "A Rapid Geometry Modeler for Conceptual Aircraft," AIAA-1996-0052, January, 1996.
[22] Carlson, H. W.; Chu, J.; Ozoroski, L. P.; and McCullers, L. A., "Guide to AERO2S and WINGDES Computer Codes for Prediction and Minimization of Drag Due to Lift," NASA TP-3637, November 1997.
[23] Sommer, S. C. and Short, B. J., "Free-Flight Measurements of Turbulent-Boundary-Layer Skin Friction in the Presence of Severe Aerodynamic Heating at Mach Numbers from 2.8 to 7.0," NACA TN-3391, 1955.
[24] Harris, Roy V., Jr., "An Analysis and Correlation of Aircraft. Wave Drag," NASA TM X-947, 1964.
[25] Wells, D. P.; Horvath, B. L.; and McCullers, L. A., "The Flight Optimization System Weights Estimation Method," NASA TM-2017-219627, vol. 1, 2017.
[26] Phoenix Integration, Inc., ModelCenter, Design Integration Software, 1715 Pratt Drive, Suite 2000, Blacksburg, VA 24060, [URL: http://www.phoenix-int.com, retrieved December, 2021].
[27] Geiselhart, K. A.; Ozoroski, L. P.; Fenbert, J. W.; Shields, E. W.; and Wu, L., "Integration of Multifidelity Multidisciplinary Computer Codes for Design and Analysis of Supersonic Aircraft," AIAA Paper 2011-465, 49th AIAA Aerospace Sciences Meeting including the New Horizons Forum and Aerospace Exposition, 4 - 7 January 2011, Orlando, Florida.
[28] Claus, R. W., et al., "Numerical Propulsion System Simulation," *Computing Systems in Engineering*, Vol. 2, No. 4, 1991, pp. 357-364.
[29] NPSS, Numerical Propulsion System Simulation, Software Package, Ver. 1.6.5, NASA, 2008.
[30] Kirby, M. R.; Mavris, D. N., "The Environmental Design Space," 26th Congress of International Council of the Aeronautical Sciences (ICAS), Anchorage, Alaska, Sep. 14-19, 2008, ICAS 2008-4.7.3.
[31] Nunez, S. L.; Tai, J. C.; and Mavris, D. N.: "The Environmental Design Space: Modeling and Performance Updates." AIAA paper 2021-1422, AIAA SciTech Forum and Exposition, 2021, doi:10.2514/6.2021-1422.
[32] Suder, K. L., Prahst, P. S., and Thorpe, S. A., "Results of an Advanced Fan Stage Operating Over a Wide Range of Speed and Bypass Ratio, Part 1: Fan Stage Design and Experimental Results," NASA TM-2011-216769, 2011.
[33] GE Aviation, "GE's Affinity: The first civil supersonic engine in 55 years – launching a new era of efficient supersonic flight," GE press release, 19 Oct. 2018 [URL: https://www.geaviation.com/press-release/business-general-aviation/ges-affinity-first-civil-supersonic-engine-55-years, retrieved December, 2021].
[34] McCullers, L. A., "Aircraft Configuration Optimization Including Optimized Flight Profiles," NASA CP-2327, April 1984, pp. 396-412.
[35] Welge, H. R., et al., "N+2 Supersonic Concept Development and Systems Integration," NASA CR-2010-216842, 2010.
[36] Anon.: "Procedure for the Calculation of Airplane Noise in the Vicinity of Airports," Soc. of Automotive Engineers SAE-AIR-1845, Warrendale, PA, 1995.
[37] Anon.: "Procedure for the Calculation of Airplane Noise in the Vicinity of Airports," Soc. of Automotive Engineers SAE-AIR-1845A, Warrendale, PA, 2012.
[38] "Recommended Method for Computing Noise Contours around Airports," Document 9911, International Civil Aviation Organization, Montreal, 2008.
[39] Lee, Cynthia, et. al, "Aviation Environmental Design Tool (AEDT) Technical Manual, Version 3b," Report No. DOT-VNTSC-FAA-19-03, Washington, D.C., Federal Aviation Administration, Sept. 2019.
[40] Lee, Cynthia, et. al, "Aviation Environmental Design Tool (AEDT) User Guide, Version 3b," Report No. DOT-VNTSC-FAA-19-02, Washington, D.C., Federal Aviation Administration, March 2019.
[41] Moulton, C. M.: "Air Force Procedure for Predicting Noise Around Airbases: Noise Exposure Model (NOISEMAP)," Rept. AL-TR-1992-0059, Accession no. AD-A255 769, Air Force Systems Command, Wright-Patterson Air Force Base, Dayton, OH, 1992.
[42] Ollerhead, J. B.: "The CAA Aircraft Noise Contour Model: ANCON Version 1," Civil Aviation Authority, Department of Safety, Environment and Engineering, Chief Scientist's Division, Civil Aviation Authority, DORA Rept. 9120, Cheltenham, England, U.K., 1992.
[43] Cavadini, L.: "STAPES (SysTem for AirPort noise Exposure Studies) Final Report," European Aviation Safety Agency Research Project EC TREN/05/ST/F2/36-2/2007-3/S07.77778, Dec. 2009.
[44] Kartyshov, O. A., and Zaporozhets, A. I.: "Metod Rascheta Konturov Aviatsionnogo Schuma [The Method of Calculating Contours of Aircraft Noise]," FGUP GosNI, ZAO TSEB GA, Moscow, 2008.
[45] Gillian, R. E., "Aircraft Noise Prediction Program User's Manual," NASA TM-84486, 1983.
[46] Zorumski, W. E., "Aircraft Noise Prediction Program Theoretical Manual, Parts 1 and 2," NASA TM-83199, 1982.
[47] Clark, B. J.: "Computer Program to Predict Aircraft Noise Levels," NASA TP-1913, 1981.
[48] Sahai, A. K., Snellen, M., Simons, D. G., and Stumpf, E., "Aircraft Design Optimization for Lowering Community Noise Exposure Based on Annoyance Metrics," *J. of Aircraft*, Vol. 54, No. 6, 2017, pp. 2257–2269.
[49] Herkes, W. H., and Reed, D. H., "Modular Engine Noise Component Prediction System (MCP) Technical Description and Assessment Document," NASA CR-2005-213526, 2005.
[50] Lopes, L. V., and Burley, C. L.: "Design of the Next Generation Aircraft Noise Prediction Program: ANOPP2," AIAA Paper 2011-2854, June 2011 (doi 10.2514/6.2011-2854).

[51] Society of Automotive Engineers, "Gas Turbine Jet Exhaust Noise Prediction," Aerospace Recommended Practice 876, Rev. F, May 2013.
[52] Henderson, B. S.; Huff, D. L.; and Berton, J. J., "Jet Noise Prediction Comparisons with Scale Model Tests and Learjet Flyover Data," AIAA Paper 2019-2768, 25th AIAA/CEAS Aeroacoustics Conference, Delft, Netherlands, 20-23 May, 2019.
[53] Henderson, B. S.; and Huff, D. L., "Scale Model Jet Tests for Learjet Flyover Data," oral presentation, AIAA SciTech Forum and Exposition, 6-10 January, 2020.
[54] Bridges, J.; and Wernet, M.: "Noise of Internally Mixed Exhaust Systems With External Plug For Supersonic Transport Applications," AIAA Paper 2021-2218 (doi 10.2514/6.2021-2218).
[55] Cluts, J.; Bridges, J.; and Podboy, G.: "Translating Phased Array Measurements of a Low-Noise Top-Mounted Propulsion Installation for a Supersonic Airliner," AIAA Paper 2019-0251 (doi 10.2514/6.2019-0251).
[56] Bridges, J.; and Wernet, M.: "PIV measurements of a low-noise top-mounted propulsion installation for a supersonic airliner," AIAA Paper 2019-0252 (doi 10.2514/6.2019-0252).
[57] Bridges, J.; Zaman, K.; and Heberling, B.: "Basics of Mixer-Ejectors for Quiet Propulsion," AIAA Paper 2020-2505 (doi 10.2514/6.2020-2505).
[58] Kontos, K. B., Janardan, B., and Gliebe, P. R., "Improved NASA-ANOPP Noise Prediction Computer Code for Advanced Subsonic Propulsion Systems, Volume 1: ANOPP Evaluation and Fan Noise Model Improvement," NASA CR-195480, 1996.
[59] Hough, J. W.; and Weir, D. S., "Aircraft Noise Prediction Program (ANOPP) Fan Noise Prediction for Small Engines," NASA CR-198300, 1996.
[60] Woodward, R. P.; Gazzaniga, J. A.; and Hughes, C. E., "Far-Field Acoustic Characteristics of Multiple Blade-Vane Configurations for a High Tip Speed Fan," NASA TM-2004-213093, May 2004.
[61] Weir, D. S., "Design and Test of Fan/Nacelle Models Quiet High-Speed Fan," NASA CR-2003-212370, July 2003.
[62] Kontos, K. B.; Kraft, R. E.; and Gliebe, P. R., "Improved NASA-ANOPP Noise Prediction Computer Code for Advanced Subsonic Propulsion Systems, Volume 2: Fan Suppression Model Development," NASA CR-202309, 1996.
[63] Emmerling, J. J., Kazin, S. B., and Matta, R. K., "Core Engine Noise Control Program. Vol. III, Supplement 1-Prediction Methods," FAA RD-74-125, III-I, March 1976.
[64] Fink, M. R., "Airframe Noise Prediction Method," FAA RD-77-29, March 1977.
[65] Herkes, W. H.; Stoker, R. W., "Wind Tunnel Measurements of the Airframe Noise of a High-Speed Civil Transport," AIAA Paper A98-16338, 36th Aerospace Sciences Meeting and Exhibit, Reno, NV, 12-15 January, 1998.
[66] Rawls, J. W.; and Yeager, J. C., "High Speed Research Noise Prediction Code (HSRNOISE) User's and Theoretical Manual," NASA CR-2004-213014, 2004.
[67] Maekawa, Z., "Noise Reduction By Screens," *Memoirs of the Faculty of Engineering*, Vol. 12, Kobe Univ., Kobe, Japan, 1966, pp. 472–479.
[68] Chien, C.; and Soroka, W. W.; "Sound propagation along an impedance plane," *J Sound and Vibration*, 1975, 43, (1), pp 9-20.
[69] Embleton, T. F. W.; Piercy, J. E.; and Daigle, G. A.; "Effective flow resistivity of ground surfaces determined by acoustical measurements," *J Acoustical Society of America*, 1983, 74, (4), pp 1239-1244.
[70] Society of Automotive Engineers, "Standard Values of Atmospheric Absorption as a Function of Temperature and Humidity," Aerospace Recommended Practice 866A, 1975.
[71] "Environmental Technical Manual, Vol. I, Procedures for the Noise Certification of Aircraft," *International Civil Aviation Organization (ICAO), Committee on Aviation Environmental Protection*, 2nd ed., Document 9501, 2015.
[72] ICAO Doc. 8168, "Aircraft Operations, vol. 1, Flight Procedures," 5th ed., 2006.
[73] FAA Advisory Circular, "Noise Abatement Departure Profiles," no. 91-53A, 1993.
[74] "Aircraft Noise and Performance (ANP) Database v2.3," [Online Database], Eurocontrol Experimental Centre, Centre du Bois des Bordes, Brétigny-sur-Orge, France, Oct. 2020, http://www.aircraftnoisemodel.org [retrieved Dec. 2021].
[75] Kirby, M. R.; and Mavris, D. N.: "Takeoff/Climb Analysis to Support AEDT APM Development Annual Report," Aviation Sustainability Center (ASCENT) Project 45 Annual Report, Pullman, WA, 2019.
[76] U.S. Code of Federal Regulations, Title 14, Chap. I, Part 25, Airworthiness Standards: Transport Category Airplanes.
[77] U.S. Code of Federal Regulations, Title 14, Chap. I, Part 91, General Operating and Flight Rules.
[78] Jackson, E.; Raney, D.; Glaab, L.; and Derry, S.: "Piloted Simulation Assessment of a High-Speed Civil Transport Configuration," NASA TP-2002-211441, 2002.
[79] Olson, E.: "Advanced Takeoff Procedures for High-Speed Civil Transport Community Noise Reduction," SAE Transactions, vol. 101, paper no. 921939, SAE International, 1992, pp. 1612-1625.
[80] McCullers, L. A., "Aircraft Configuration Optimization Including Optimized Flight Profiles," NASA CP-2327, April 1984, pp. 396-412.
[81] Hassan, M.; Pfaender, H.; and Mavris, D.: "Design Tools for Conceptual Analysis of Future Commercial Supersonic Aircraft," AIAA paper 2020-2620, 2020 (doi: 10.2514/6.2020-2620).
[82] Kirby, M. R.; and Mavris, D. N.: "Noise-Power-Distance Re-Evaluation Annual Report," Aviation Sustainability Center (ASCENT) Project 43 Annual Report, Pullman, WA, 2020.